J Mater Sci (2009) 44:1881–1888
DOI 10.1007/s10853-008-3223-8

The mechanical and viscoelastic properties of SSBR vulcanizates filled with organically modified montmorillonite and silica

Hong Li · Jin Sun · Yihu Song · Qiang Zheng

Received: 26 September 2008 / Accepted: 22 December 2008 / Published online: 3 February 2009

Abstract The mechanical and the dynamic rheological behavior of solution-polymerized styrene butadiene rubber (SSBR) filled with compounding fillers organic montmorillonite (OMMT)/silica (SiO_2) were studied. The mechanical properties of the vulcanizates could be improved by incorporation of low OMMT contents, and the best reinforcement effect appeared when 7 phr (parts per hundred rubber) OMMT was added. Moreover, due to the formation of the exfoliated silicate platelet in the matrix, a strong cooperative reinforcement effect to the vulcanizate could be gained for the vulcanizate containing 7 phr OMMT and 20 phr SiO_2. Incorporation of SiO_2 up to 50 phr to the vulcanizates with or without OMMT resulted in marked reinforcement effect, and the best mechanical properties were obtained for 7 phr OMMT filled composites. On the other hand, compounding fillers OMMT/SiO_2 significantly influences the dynamic mechanical behavior of the vulcanizates. It was found that the compounding filler with a certain composition facilitated preparing SSBR vulcanizates with optimized wet traction, rolling resistance, and strength properties.

H. Li · J. Sun · Y. Song · Q. Zheng (✉)
Key Laboratory of Macromolecular Synthesis and Functionalization, Ministry of Education, Zhejiang University, Hangzhou 310027, China
e-mail: zhengqiang@zju.edu.cn; zhengqiang@zjuem.zju.edu.cn

H. Li · J. Sun · Y. Song · Q. Zheng
National Engineering Research Center for Compounding and Modification of Polymeric Materials, Guiyang 550025, China

H. Li
School of Material and Architectural Engineering, Guizhou Normal University, Guiyang 550014, China

Introduction

The use of silica (SiO_2) as a reinforcing filler, in place of conventional carbon black (CB), has been preferentially selected for preparing vulcanizates with a unique combination of tear strength, abrasion resistance, age resistance, and adhesion properties. A combination of SiO_2 and CB is highly efficient to lower the rolling loss and to improve the wet skid resistance so as to produce green tires with limited energy consumption and CO_2 emission from automobiles. Such tires can reduce fuel consumption by approximately 6% and reduce emission of pollutants [1, 2].

It is known that clay could be used as a promising reinforcing agent in the rubber industry if it is dispersed on a nanometer level by mean of some special methods [3]. Organically modified montmorillonite (OMMT) is usually employed to prepare nanocomposites possessing much higher mechanical properties and gas barrier properties [4–6]. Preparation, structure, and properties of rubber/organoclay nanocomposites have been investigated for a number of rubber matrices, e.g., natural rubber (NR) [7–12], butadiene rubber (BR) [13], NBR [3, 4, 14–18], styrene-butadiene rubber (SBR) [3, 15, 19–25], ethylene propylene diene terpolymer (EPDM) [26–29], chlorobutyl rubber [30], silicone rubber [6, 10, 31–33], fluoroelastomer [34–36], and ethylene acrylate rubber (EAR) [37].

SBR/clay nanocomposites have been prepared by using latex co-coagulation [19, 20, 38, 39], solution compounding [40], melt compounding [41], and in situ living copolymerization methods [24]. In the exfoliated SBR nanocomposite, the reinforcement effect of 4 wt% allylamine modified clay is equivalent to at least 10 wt% CB [38]. In case of 20 phr clay loadings, tensile strength of SBR nanocomposite is 6 times higher than that of the conventional SBR/clay composite [19].

Traditional fillers can be used to further improve the mechanical properties of rubber nanocomposites. Moreover, loading of 4 phr OMMT can significantly improve tensile strength of SBR filled with CB, SiO_2 or china clay [42]. Incorporation of 4–5 phr nanodispersed clay can dramatically improve the flex-fatigue life of CB filled SBR by improving the hysteresis and tearing energy without influencing degree of crosslinking [43].

To our knowledge, there have been no reports on the effect of OMMT and SiO_2 as compounding filler on structure and properties of solution-polymerized styrene butadiene rubber (SSBR). The aim of this article is to probe the influence of OMMT and its combination with SiO_2 on mechanical and dynamic mechanical behaviors of the melt compounded SSBR composites vulcanized using sulfur vulcanization system.

Experimental

Materials and sample preparation

Solution-polymerized styrene butadiene rubber (SSBR, PR1205) containing 25% styrene and 35% *cis*-1,4 structure was provided by Qimei Co., China. Silica (SiO_2, Ultrasil VN3 GR, pH 5.4–7.0, surface area 175 m^2/g, average diameter 20 nm) was a product of DEGUSSA Co., Germany. Alkyl ammonium modified montmorillonite (OMMT) was a product of Zhejiang Fenghong Clay Chemicals CO., Ltd., China. Silane coupling agent bis-(triethoxysilylpropyl)-tetrasulfide (TESPT) was purchased from Nanjing Crompton Shuguang Organosilicon Specialties Co., China. Stearate, wax, zinc oxide, antioxidant *N*-(1,3-Dimethylbutyl)-*N*′-phenyl-*p*-phenylenediamine (6PPD), sulfur, accelerator *N*-cyclohexy-2-benzothiazolesul fenamide (CBS), and 1,3-Diphenylguanidine (DPG) were obtained from Shanghai Jinghui Chem. Techn. Co., China.

Rubber composites were formulated with 2.5 phr (parts per hundred rubber) zinc oxide, 1 phr stearate, 2 phr antioxidant, 1.5 phr wax, and various loadings of TESPT, OMMT, SiO_2 or both fillers. OMMT, SiO_2, or both fillers were mixed physically with TESPT first at room temperature. The ratio of TESPT to filler remained constant at 0.14. The resulting mixture was mixed with SSBR and other ingredients on a two-roll mill at 50 °C, followed by a further mixing in a HAAKE Rheometer (Thermo Haake Polylab System, Germany) at 150 °C at 30 rpm for 10 min. Sulfur was then added into the compound using a two-roll mill at 50 °C. The resulting compound was vulcanized at 160 °C and 10 MPa for 10 min. The composites were designated as SSBR-M*x*Si*y* with *x* and *y* presenting the amount of OMMT and SiO_2, respectively, in phr.

Dynamic rheological measurements

The curing characteristics of the uncured compounds were determined on an Advanced Rheometeric Expansion System (ARES, TA Instrument, USA) using parallel plate mode. The time sweeps were performed under conditions of strain being 1%, frequency being 1 rad s^{-1} and temperature being 160 °C.

X-ray diffraction (XRD) studies

For the characterization of OMMT and rubber composites, XRD studies were performed on a Rigaku D/max-III B diffractometer (Rigaku Co., Japan) with the Cu $K\alpha$ radiation at room temperature from 1 to 10° (2θ). The interspace distance d of OMMT in the vulcanized composites was calculated according to Bragg's equation.

Mechanical properties

Tensile strength and elongation at break were measured on an electronic multifunctional tensile testing machine (SANA-CMT4204, Shenzhen Sans Testing Machine Co., China) under tensile rate of 500 mm min^{-1} at 25 ± 2 °C. The maximum load of the tensile machine was 100 N. The data were reported as average values from three different specimens for each product.

Dynamic mechanical analysis (DMA)

Dynamic mechanical analysis (DMA) was performed on a TA Q800 DMA (TA Instruments, USA) using single cantilever mode for the vulcanized composites. The measurements were performed under conditions of strain being 1%, frequency being 1 rad s^{-1}, heating rate being 3 °C min^{-1} and temperature range being from −100 to 120 °C.

Morphological observation

Ultra-thin sections of the unfilled SSBR and the filled vulcanizates with a thickness of 200–300 nm were obtained by cryogenic ultramicrotoming. The filler dispersion was observed by transmission electron microscopy (TEM, JEM-1230, Electron Co., Japan).

Results and discussion

Vulcanization characteristics

Figure 1 gives the effect of OMMT content on the vulcanization characteristics of SSBR, which graphically

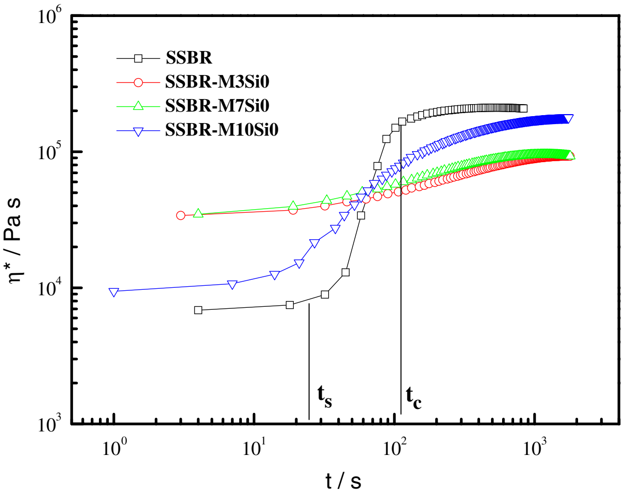

Fig. 1 Complex viscosity (η^*) as a function of time at 1% strain and 1 rad s^{-1} for SSBR compounds. The vertical lines indicate the characteristic times t_s and t_c

presented as complex viscosity (η^*) as a function of time (t). It can be seen that the compounds with different OMMT loadings show similar behavior of convenient vulcanization characteristic. In general, η^* remains unvaried at t below a characteristic time t_s, At $t > t_s$, η^* increases significantly with t, corresponding to the cross-linking reaction of SSBR. For a long time above another characteristic time t_c, η^* increases only slowly. The unfilled SSBR shows η^* values lower than those of the filled compounds at $t < t_s$, revealing the reinforcement effect of OMMT to uncured SSBR compounds. The unfilled SSBR shows η^* increment between t_s and t_c faster than those of the filled compounds, suggesting that OMMT causes pre-vulcanization during the compounding process. The SSBR-M3Si0 and SSBR-M7Si0 samples exhibit similar curing characteristic being slower than those of SSBR and SSBR-M10Si0. The η^* values of SSBR-M3Si0 and SSBR-M7Si0 are higher than those of SSBR and SSBR-M10Si0 when $t < t_s$ while the reverse can be observed at $t > t_c$. This behavior could be ascribed to the delay of vulcanization because of the partial absorption of curing agent and CBS cure accelerator on the surface of OMMT.

XRD-ray analysis

Figure 2 shows the XRD patterns for the OMMT as well as the SSBR composites. The XRD pattern of OMMT reveals two intense diffraction peaks at $2\theta = 2.38°$ and 4.79°, respectively, corresponding to interlayer distances of 3.69 nm and 1.85 nm given in Table 1, higher than that of 1.22 nm for unmodified Na-MMT [44]. The appearance of the two diffraction peaks in OMMT may be due to the lack of interlayer symmetrical arrangement of modified clay [45].

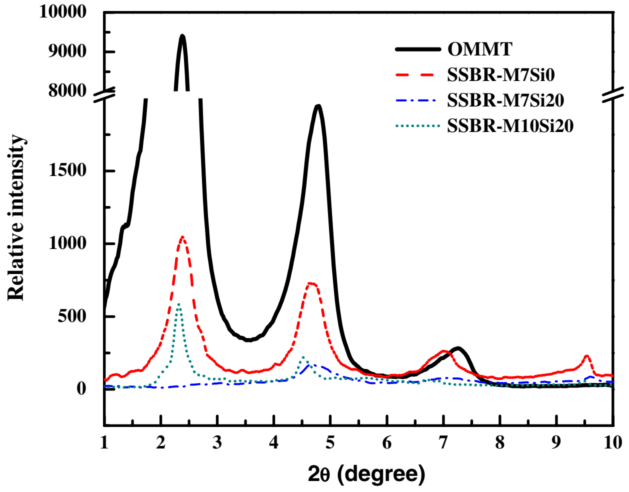

Fig. 2 XRD spectra of OMMT and SSBR nanocomposites

Table 1 Gallery spacings of OMMT and SSBR composites

Sample	d_{001}/nm)	d_{002}/nm
OMMT	3.69	1.85
SSBR-M7Si0	3.69	1.93
SSBR-M7Si20	Exfoliated	1.88
SSBR-M10Si20	3.81	1.94

The SSBR-M7Si0 composite shows two diffraction peaks very close to those of the OMMT, suggesting that the melt compounding leads to intercalation of SSBR chains to OMMT interlayer. The SSBR-M7Si20 composite shows only one diffraction peak at 1.88 nm and its intensity is considerably low. On the other hand, the diffraction peak in the range of 1.0–3.5° does not appear, implying that most of OMMT forms exfoliated structure in the SSBR matrix containing 20 phr SiO_2. Except for the weak diffraction peak at 1.94 nm, the peak at 3.81 nm appears again in SSBR-M10Si20 composite. This composite probably forms the mixed structure of exfoliation and intercalation due to the high OMMT content. Besides the modification of MMT [46] and the type of vulcanization accelerators [47], the intercalation is related to the processing conditions [48]. The results shown in Fig. 2 indicate that SiO_2 is conducive to promoting the intercalation of SSBR chain to the gallery of OMMT and a certain ratio of SiO_2 to OMMT may facilitate formation of completely exfoliated OMMT platelets dispersed well in the SSBR matrix.

Morphological observation

Figure 3 gives TEM images of the vulcanizates. SSBR-M7Si0 contains prolate, ellipsoidal, or spherulite MMT

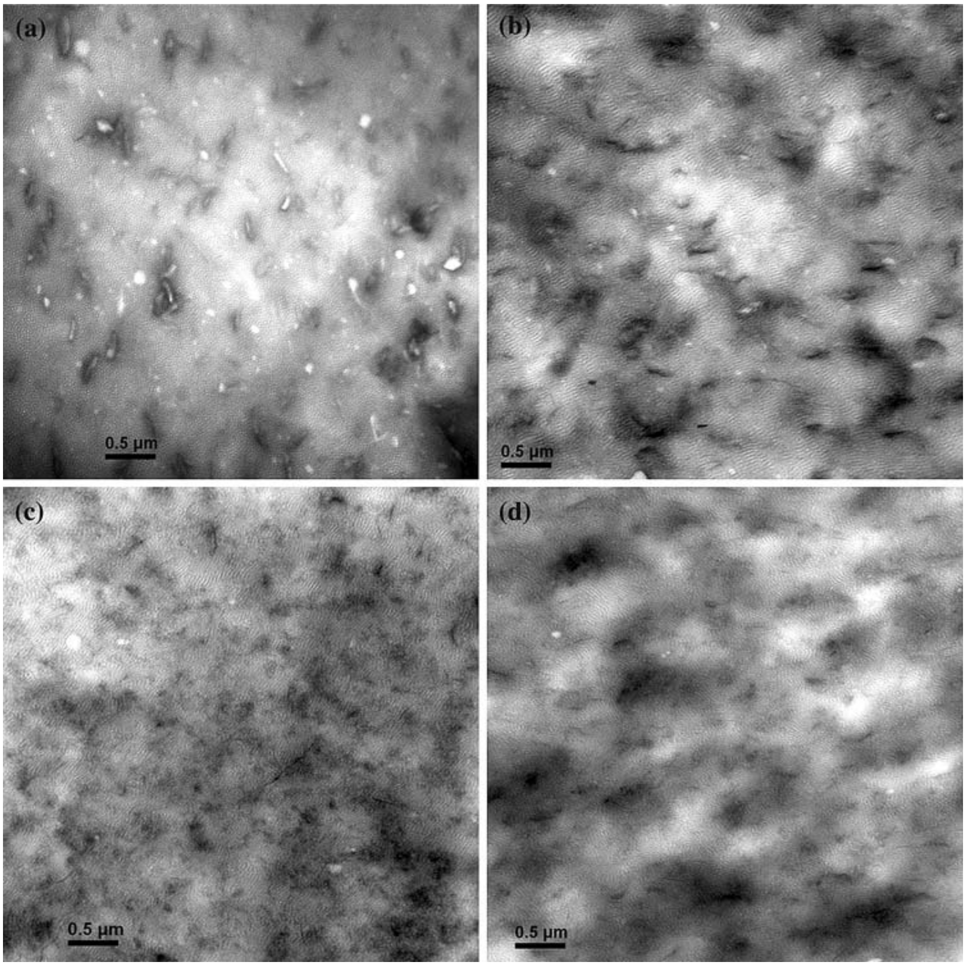

Fig. 3 TEM images of SSBR-M7Si0 (**a**), SSBR-M10Si0 (**b**), SSBR-M7Si20 (**c**), and SSBR-M10Si20 (**d**) vulcanizates

aggregates in the size less than 190 nm, which are well dispersed in rubbery matrix (Fig. 3a). The size of MMT aggregates becomes larger in SSBR-M10Si0 (Fig. 3b). The presence of 20 phr SiO_2 is unfavorable to the observation of the morphology of MMT in SSBR-M7Si20 and SSBR-M10Si20. Nevertheless, the TEM images reveals that the fillers are well dispersed SSBR-M7Si20 (Fig. 3c) whereas the dispersion becomes poor in SSBR-M10Si20 (Fig. 3d). The filler aggregation in SSBR-M10Si20 is more severe than that in SSBR-M10Si0.

Mechanical properties analysis

Figure 4 presents tensile strength and elongation at break as a function of OMMT loading for the OMMT filled SSBR vulcanizates (SSBR-M*x*Si0). It can be seen that tensile strength and elongation at break increase sharply from 3 MPa and 738% for the unfilled vulcanizate to 6.27 MPa and 956% for the vulcanizate containing 7 phr OMMT, respectively. Further loading OMMT to 10 phr leads to a reduction in tensile strength and elongation at break. Moreover, at high loadings, the poor dispersion of OMMT results in formation of aggregates in the rubber matrix, which is responsible for the degradation in mechanical properties. It is worth noting that the

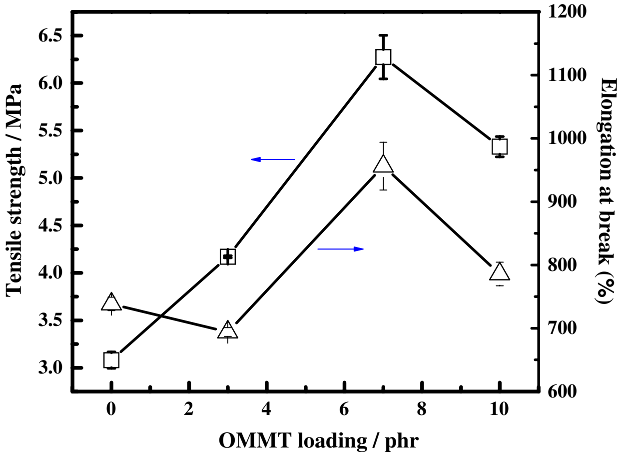

Fig. 4 Tensile strength and elongation at break as a function of the OMMT content for the vulcanized composites without SiO_2

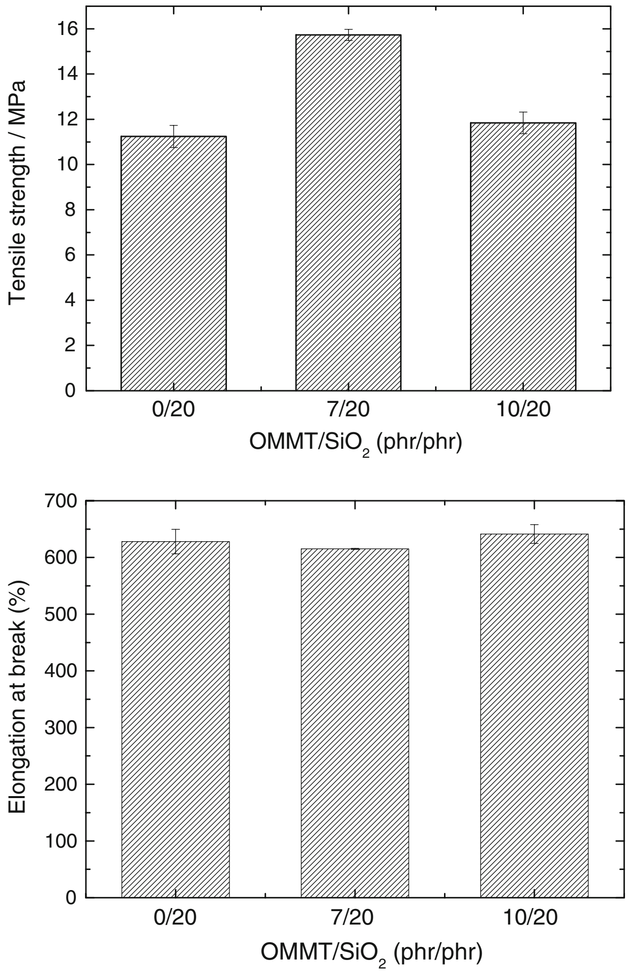

Fig. 5 Influence of OMMT loading on tensile strength and elongation at break for the vulcanizates filled with 20 phr SiO_2

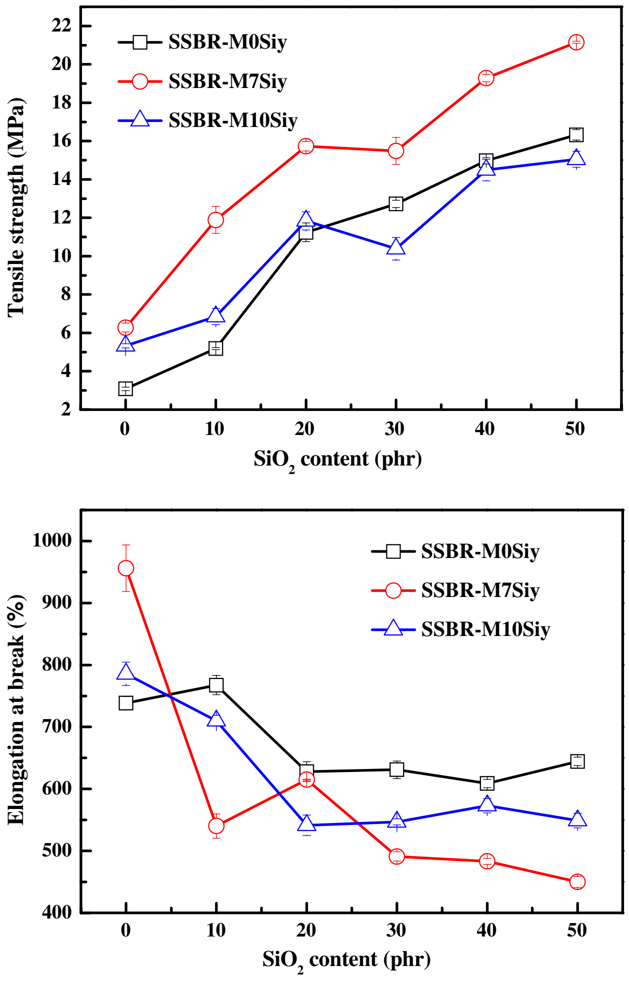

Fig. 6 Tensile strength and elongation at break as a function of SiO_2 loading for the vulcanizates with 0 phr, 7 phr, and 10 phr OMMT, respectively

vulcanized composite containing 7 phr OMMT exhibits the best mechanical properties.

Figure 5 shows influence of OMMT loading on tensile strength and elongation at break for the vulcanizates filled with 20 phr SiO_2 (SSBR-M*x*Si20). Strong interactions between SiO_2 particles and SBR result in the formation of bound rubber, which is involved in the high level of reinforcement [49]. The SSBR-M7Si20 vulcanizate containing 7 phr OMMT and 20 phr SiO_2 shows the exfoliated structure, and as a result, its tensile strength is higher than that of those containing SSBR-M0Si20 and SSBR-M10Si20 vulcanizates. On the other hand, elongation at break does not vary markedly with respect to OMMT loading. Addition of 7 phr OMMT can significantly improve tensile strength of the 20 phr SiO_2 filled vulcanizate, the corresponding value being 5 times higher than that of the unfilled SSBR vulcanizate.

Figure 6 shows tensile strength and elongation at break as a function of SiO_2 loading for the SSBR-M0Si$_y$, SSBR-M7Si$_y$, and SSBR-M10Si$_y$ vulcanizates. Table 2 lists the values of mechanical properties for SSBR and its composites. For the vulcanizates without SiO_2, moduli at 100, 200, and 300% elongation increase with increase OMMT loading and reach to the maximum at 7 phr OMMT. The same trend can be found for the vulcanizates

Table 2 Mechanical properties of vulcanized SSBR composites

Sample	Tensile strength (MPa)	Elongation at break (%)	Tensile modulus (MPa)		
			100%	200%	300%
SSBR	3.1	738	0.20	0.29	0.37
SSBR-M3Si0	4.2	693	0.32	0.50	0.65
SSBR-M7Si0	6.3	956	0.55	0.87	1.08
SSBR-M10Si0	5.3	785	0.50	0.76	1.01
SSBR-M0Si20	11.2	594	0.39	0.63	0.81
SSBR-M7Si20	15.7	615	0.62	0.92	1.13
SSBR-M10Si20	11.8	641	0.58	0.82	1.01

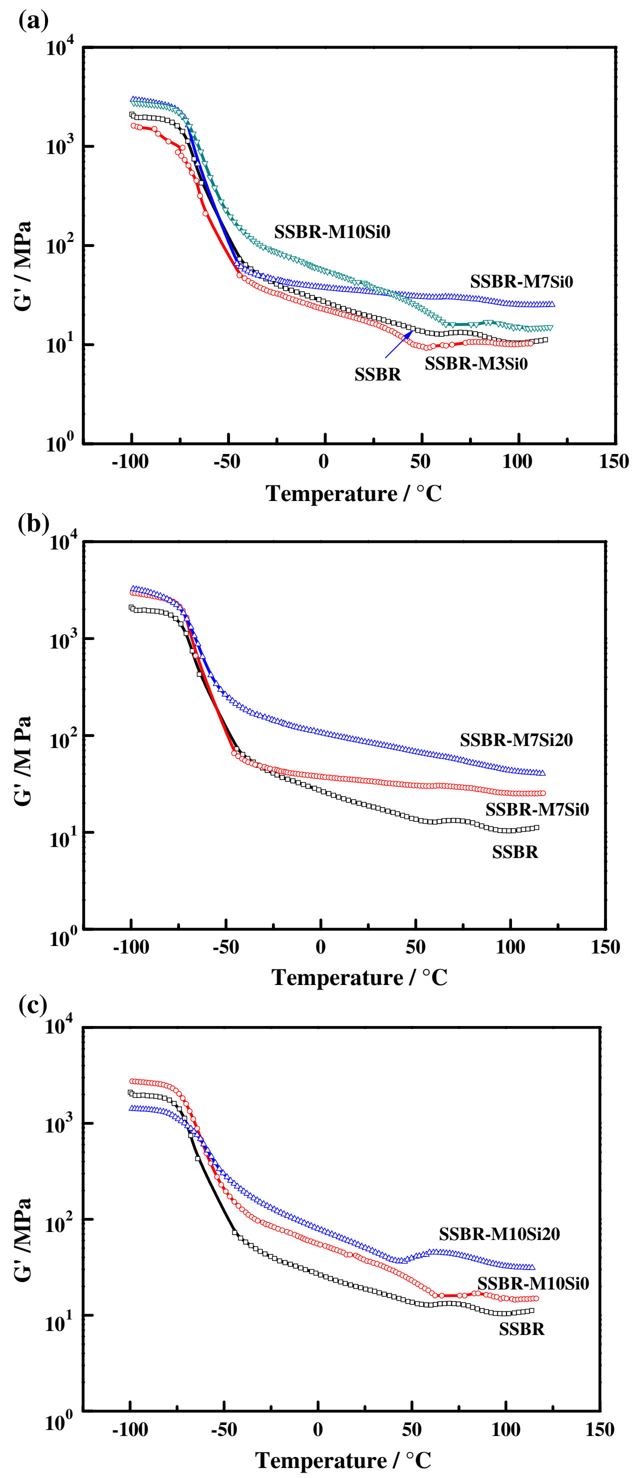

Fig. 7 Dynamic storage modulus (G') as a function of temperatures at 1% strain and 1 rad s^{-1} for SSBR filled with different fillers

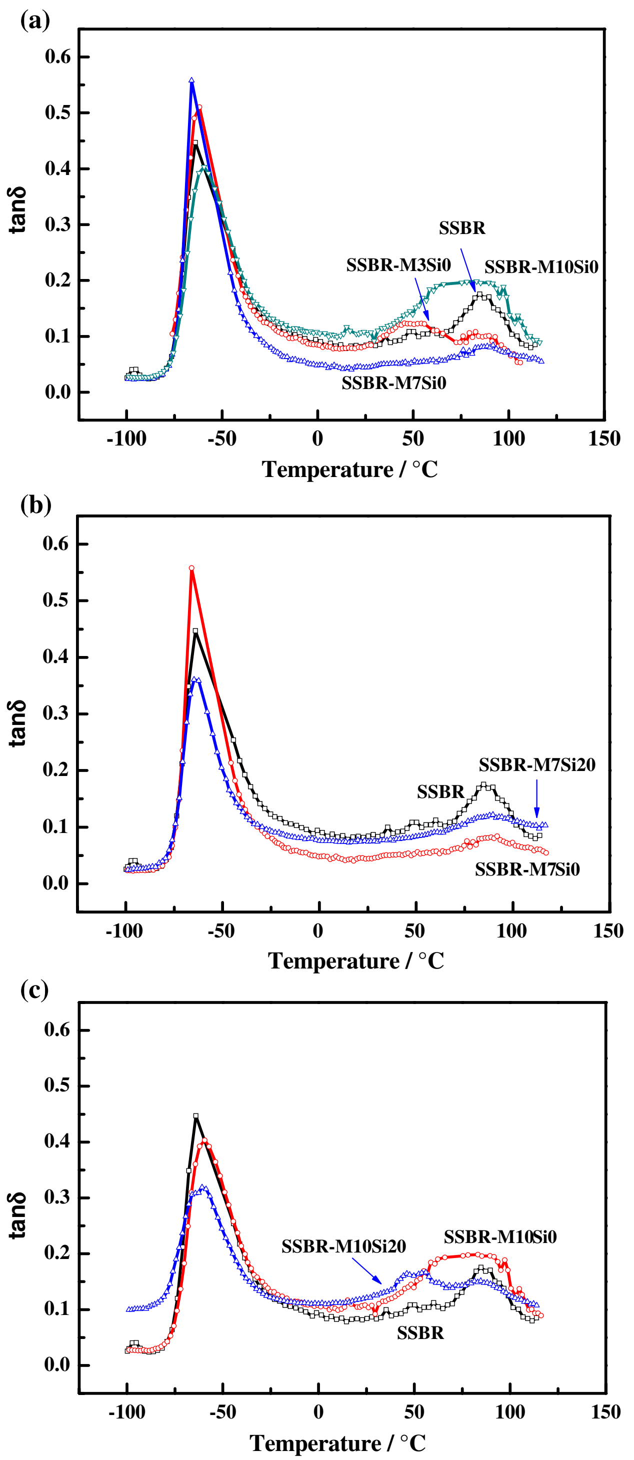

Fig. 8 Dynamic loss tangent (tanδ) as a function of temperatures at 1% strain and 1 rad s^{-1} for SSBR filled with different fillers

containing 20 phr SiO_2. In general, for filled rubber vulcanizates, the tensile strength increases, while elongation at break decreases significantly with increase of SiO_2 loading up to 50 phr. The reinforcement effect of SiO_2 to the vulcanizates filled with 7 phr OMMT is superior to that of those filled with 0 phr and 10 phr OMMT. Due to the OMMT aggregation, the reinforcement effect of adding SiO_2 on the vulcanizates containing 10 phr OMMT is comparable to that of those without OMMT. Furthermore, elongation at break of the vulcanizates filled with 10 phr

Table 3 Dynamic mechanical properties at various temperatures for vulcanized SSBR composites

Sample	T_{g1} (°C)	tanδ at T_{g1}	T_{g2} (°C)	tanδ at T_{g2}	tanδ (0 °C)	tanδ (60 °C)
SSBR	−64	0.447	84	0.176	0.094	0.112
SSBR-M3Si0	−62	0.510	86	0.101	0.084	0.110
SSBR-M7Si0	−65	0.557	84	0.081	0.048	0.057
SSBR-M10Si0	−60	0.403	83	0.198	0.108	0.182
SSBR-M7Si20	−64	0.360	84	0.117	0.076	0.091
SSBR-M10Si20	−60	0.319	85	0.150	0.111	0.148

OMMT is slightly higher than that of those without OMMT. It is noted that addition of 7 phr OMMT shows the best reinforcement effect for SiO_2 filled SSBR vulcanizates.

Dynamic rheological properties

Figures 7 and 8 show the influence of filler type and loading on dynamic storage modulus (G') and loss tangent (tanδ) as a function of temperature for SSBR vulcanizates. In comparison with the unfilled SSBR vulcanizate, SSBR vulcanizates filled with 7 phr and 10 phr OMMT show an increase of G' in temperatures above −50 °C. On the other hand, incorporation of 3 phr OMMT causes a slight reduction in G', which could be related to the poor dispersion of OMMT in the rubbery matrix. The dispersion of OMMT in the SSBR matrix strongly influences G' with variation of temperature, and G' of the SSBR-M7Si0 vulcanizate does not vary markedly in temperatures above −50 °C, while that of the SSBR-M10Si0 vulcanizate decreases notably until 63 °C (Fig. 7a). For the vulcanizates containing 7 phr and 10 phr OMMT, incorporation of 20 phr SiO_2 further increase G' at temperatures above −50 °C, which is constant with the variation in tensile strength (Fig. 7b, c).

The glass transition temperature (T_g) of SSBR vulcanizate is located at −64 °C, which is lower than that of pure SBR vulcanizate at −39 °C [50]. There appears a glass transition peak centered at −64 °C and a high-temperature relaxation peak at 84 °C in tanδ curve of the unfilled SSBR vulcanizate (Fig. 8a). The week relaxation peak at 84 °C is responsible for the glass transition of short polystyrene (PS) blocks, whose position is lower than T_g of bulk PS phase. It is emphasized that introduction of OMMT and SiO_2 could hardly influence the position of T_g of crosslinked SSBR. The SSBR-M3Si0 vulcanizate exhibits an additional transition peak at 50 °C, which is related to the breakdown and reformation of the filler network [51, 52]. For the SSBR-M10Si0 vulcanizate filled with 10 phr OMMT, this transition shifts to high temperatures and merges into the glass transition of the short PS blocks, giving rise to a broader peak in temperature range from 50 °C to 120 °C. Furthermore, addition of 20 phr SiO_2 to the 10 phr OMMT filled vulcanizates leads to the visualization of a distinct transition peak at 50 °C (Fig. 8c). The peak induced by the relaxation of the filler network is absent in the vulcanizate filled with 7 phr OMMT exhibiting the best mechanical properties (Fig. 8a). Otherwise, addition of 20 phr SiO_2 to this vulcanizate can increase the tanδ values at high temperature (Fig. 8b).

Table 3 lists values of T_g and tanδ in given temperatures. The tanδ values at 0 °C and 60 °C reflect the wet traction and the rolling resistance, respectively [53]. A high tanδ value at 0 °C facilitates a good wet traction property, while a low tanδ value at 60 °C corresponds to a good rolling resistance property after vulcanization. The tanδ values at 0 °C and 60 °C are 0.094 and 0.112, respectively, for the SSBR. The highest tanδ value at 0 °C is 0.111 for the SSBR-M10Si20 and the low tanδ value at 60 °C is 0.057 for the SSBR-M7Si0, which means the wet traction resistance can be improved by using OMMT/SiO_2 compounding fillers. However, tanδ value at 60 °C falls about 50% with the addition of 7 phr OMMT, and the vulcanizate with a further addition of 20 phr SiO_2 exhibits a tanδ value at 60 °C, still lower than that of the SSBR vulcanizate without filler. The results suggest that the OMMT/SiO_2 compounding filler with a certain composition is helpful to prepare SSBR vulcanizates with the optimized wet traction, rolling resistance, and strength properties.

Conclusions

The presence of SiO_2 facilitates the intercalation of SSBR chains into the gallery of OMMT to form exfoliated composites during melt compounding. OMMT filled SSBR vulcanizates display superior mechanical properties compared to the gum vulcanizate, and the vulcanizate containing 7 phr OMMT shows the highest value of tensile strength and elongation at break. SiO_2 show a marked reinforcement effect on SSBR vulcanizates with and without OMMT filling. Meanwhile, SiO_2 promotes the dispersion of OMMT in the rubber. The OMMT/SiO_2 compounding filler significantly influences the dynamic mechanical behavior of the vulcanizates. The compounding filler with a certain composition is conducive to preparing SSBR vulcanizates with the optimized wet traction, rolling resistance, and strength properties.

References

1. Bokobza L, Chauvin JP (2005) Polymer 46:4144
2. Gauthier C, Reynaud E, Vassoille R, Ladouce-Stelandre L (2004) Polymer 45:2761
3. Wang YZ, Zhang LQ, Tang CH, Yu DS (2000) J Appl Poly Sci 78:1879
4. Han M, Kim H, Kim E (2006) Nanotechnology 17:403
5. Yeh MH, Hwang WS, Chang YC (2005) Jpn J Appl Phys 1 44:6847
6. Wang SH, Zhang Y, Ren WT, Zhang YX, Lin HF (2005) Polym Test 24:766
7. Arroyo M, Lopez-Manchado MA, Herrero B (2003) Polymer 44:2447
8. Arroyo M, Lopez-Manchado MA, Valentin JL, Carretero J (2007) J Compos Sci Tech 67:1330
9. Teh PL, Ishak ZAM, Hashim AS, Karger-Kocsis J, Ishiaku US (2006) J Appl Polym Sci 100:1083
10. Wang JC, Chen YH (2008) J Appl Polym Sci 107:2059
11. Jurkowska B, Jurkowski B, Oczkowski M, Pesetskii SS, Koval V, Olkhov YA (2007) J Appl Polym Sci 106:360
12. Valadares LF, Leite CAP, Galembeck F (2006) Polymer 47:672
13. Hwang WG, Wei KH, Wu CM (2006) Polym Eng Sci 46:80
14. Wang YQ, Wu YP, Zhang HF, Zhao W, Wang CX, Zhang LQ (2005) Polym J 37:154
15. Sadhu S, Bhowmick A (2005) J Mater Sci 40:1633. doi: 10.1007/s10853-005-0663-2
16. Liu L, Jia DM, Luo YF, Guo BC (2006) J Appl Polym Sci 100:1905
17. Kato M, Tsukigase A, Tanaka H, Usuki A, Inai I (2006) J Polym Sci A 44:1182
18. Kader MA, Kim K, Lee YS, Nah C (2006) J Mater Sci 41:7341. doi:10.1007/s10853-006-0792-2
19. Wu YP, Wang YQ, Zhang HF, Wang YZ, Yu DS, Zhang LQ, Yang J (2005) Compos Sci Tech 65:1195
20. Abdollahi M, Rahmatpour A, Aalaie J, Khanli HH (2007) E-Polymers, Article no. 074
21. Zhang ZJ, Zhang LN, Li Y, Xu HD (2006) J Appl Polym Sci 99:2273
22. Das A, Jurk R, Stockelhuber KW, Engelhardt T, Fritzsche J, Kluppel M, Heinrich G (2008) J Macromol Sci A 45:144
23. Jia QX, Wu YP, Lu M, He SJ, Wang YQ, Zhang LQ (2008) Compos Interface 15:193
24. Zhang ZJ, Zhang LN, Li Y, Xu HD (2005) Polymer 46:129
25. Zhang HF, Wang YQ, Wu YP, Zhang LQ, Yang J (2005) J Appl Polym Sci 97:844
26. Acharya H, Srivastava SK, Bhowmick AK (2006) Polym Eng Sci 46:837
27. Mohammadpour Y, Katbab AA (2007) J Appl Polym Sci 106:4209
28. Zheng H, Zhang Y, Peng ZL, Zhang YX (2005) Polym Polym Compos 13:53
29. Ma Y, Wu YP, Wang YQ, Zhang LQ (2006) J Appl Polym Sci 99:914
30. Sridhar V, Tripathy DK (2006) J Appl Polym Sci 101:3630
31. Yang L, Hu Y, Lu HD, Song L (2006) J Appl Polym Sci 99:3275
32. Wang JC, Chen YH, Jin QQ (2006) High Perform Polym 18:325
33. Wang SJ, Long CF, Wang XY, Li Q, Qi ZN (1998) J Appl Polym Sci 69:1557
34. Maiti M, Bhowmick AK (2006) J Polym Sci B 44:162
35. Maiti M, Bhowmick AK (2006) Polymer 47:6156
36. Maiti M, Mitra S, Bhowmick AK (2008) Polym Degrad Stabil 93:188
37. Mathew G, Rhee JM, Lee YS, Park DH, Nah C (2008) J Indus Eng Chem 14:60
38. Manchado MAL, Arroyo M, Herrero B, Vicente R (2004) Bol Soc Esp Ceram V 43:514
39. Kim W, Kang BS, Cho SG, Ha CS, Bae JW (2007) Compos Interface 14:409
40. Sadhu S, Bhowmick AK (2004) J Appl Polym Sci 92:698
41. Wu YP, Ma Y, Wang YQ, Zhang LQ (2004) Macromol Mater Eng 289:890
42. Maiti M, Sadhu S, Bhowmick AK (2005) J Appl Polym Sci 96:443
43. Wu YP, Zhao W, Zhang LQ (2006) Macromol Mater Eng 291:944
44. Wan CY, Dong W, Zhang YX, Zhang Y (2008) J Appl Polym Sci 107:650
45. Akelah A, Rehab A, Agag T, Betiha M (2007) J Appl Polym Sci 103:3739
46. Gatos KG, Karger-Kocsis J (2005) Polymer 46:3069
47. Usuki A, Tukigase A, Kato M (2002) Polymer 43:2185
48. Dennis HR, Hunter DL, Chang D, Kim S, White JL, Cho JW, Paul DR (2001) Polymer 42:9513
49. Leblanc JL (2000) J Appl Polym Sci 78:1541
50. Derakhshandeh B, Shojaei A, Faghihi M (2008) J Appl Polym Sci 108:3808
51. Schon F, Thomann R, Gronski W (2002) Macromol Symposia 189:105
52. Lu YL, Li Z, Yu ZZ, Tian M, Zhang LQ, Mai YW (2007) Compos Sci Tech 67:2903
53. Choi SS (2001) J Appl Polym Sci 79:1127